

## Original Article

# Proliferation and cell death of human glioblastoma cells after carbon-ion beam exposure: morphologic and morphometric analyses

Takuma Oishi,<sup>1,5</sup> Atsushi Sasaki,<sup>1</sup> Nobuyuki Hamada,<sup>2,5,6</sup> Shogo Ishiuchi,<sup>3,5</sup>  
Tomoo Funayama,<sup>6</sup> Tetsuya Sakashita,<sup>6</sup> Yasuhiko Kobayashi,<sup>2,5,6</sup>  
Takashi Nakano,<sup>4,5</sup> Yoichi Nakazato<sup>1,5</sup>

<sup>1</sup>Departments of Human Pathology, <sup>2</sup>Quantum Biology, <sup>3</sup>Neurosurgery, and <sup>4</sup>Radiation Oncology, and <sup>5</sup>The 21st Century Center of Excellence (COE) program, Gunma University Graduate School of Medicine, Gunma, Japan, <sup>6</sup>Microbeam Radiation Biology Group, Japan Atomic Energy Agency (JAEA), Gunma, Japan

**Histological analyses of glioblastoma cells after carbon-ion exposure are still limited and ultrastructural characteristics have not been investigated in detail. Here we report the results of morphological and morphometric analyses of a human glioblastoma cell line, CGNH-89, after ionizing radiation to characterize the effect of a carbon-beam on glioblastoma cells. Using CGNH-89 cells exposed to 0–10 Gy of X-ray (140kVp) or carbon-ions (18.3 MeV/nucleon, LET = 108 keV/μm), we performed conventional histology and immunocytochemistry with MIB-1 antibody, transmission electron microscopy, and computer-assisted, nuclear size measurements. CGNH-89 cells with a G to A transition in codon 280 in exon 8 of the TP53 gene had nuclei with pleomorphism, marked nuclear atypia and brisk mitotic activity. After carbon-ion and X-ray exposure, living cells showed decreased cell number, nuclear condensation, increased atypical mitotic figures, and a tendency of cytoplasmic enlargement at the level of light microscopy. The deviation of the nuclear area size increased during 48 hours after irradiation, while the small cell fraction increased in 336 hours. In**

**glioblastoma cells of the control, 5 Gy carbon-beam, and 10 Gy carbon-beam, and MIB-1 labeling index decreased in 24 hours (12%, 11%, 7%, respectively) but increased in 48 hours (10%, 20%, 21%, respectively). Ultrastructurally, cellular enlargement seemed to depend on vacuolation, swelling of mitochondria, and increase of cellular organelles, such as the cytoskeleton and secondary lysosome. We could not observe apoptotic bodies in the CGNH-89 cells under any conditions. We conclude that carbon-ion irradiation induced cell death and senescence in a glioblastoma cell line with mutant TP53. Our results indicated that the increase of large cells with enlarged and bizarre nuclei, swollen mitochondria, and secondary lysosome occurred in glioblastoma cells after carbon-beam exposure.**

**Keywords:** carbon-beam, glioblastoma, MIB-1, morphometry, Ultrastructure

## INTRODUCTION

Glioblastoma is the most frequent and the most malignant neoplasm with predominant astrocytic differentiation of the primary glial tumors. Due to their invasive nature, glioblastomas cannot be completely resected despite progress in radio/chemotherapy, and the overall survival of patients with glioblastoma remains extremely poor as follows; median survival time with primary and secondary glioblastoma is 4.7 months and 7.8 months, respectively.<sup>1,2</sup>

---

Correspondence: Atsushi Sasaki, MD, PhD, Department of Human Pathology, Gunma University Graduate School of Medicine, 3-39-22 Showa-machi, Maebashi, Gunma, 371-8511, Japan. E-mail: [achie@med.gunma-u.ac.jp](mailto:achie@med.gunma-u.ac.jp)

Received ; revised; accepted

Recently, high linear energy transfer (LET) charged particle therapy with carbon-ions has been of interest in the treatment of glioblastoma because of better dose localization in the tumor volume and greater biologic effectiveness. Clinically, combined therapy using X-ray radiotherapy, carbon-ion radiotherapy (CRT) and chemotherapy showed the potential efficacy of CRT for glioblastoma in terms of the improved median survival time (26 months) in patients who received higher carbon-beam doses.<sup>3</sup> In a previous experiment using human glioblastoma xenografts, the incidence of apoptosis increased more than 3-fold after carbon-ion irradiation in comparison with photon.<sup>4</sup>

Morphologically, radiation-induced cell death is now mainly classified into three modes: (1) apoptosis, type-I cell death, caspase-dependent programmed cell death (PCD); (2) autophagic cell death, type-II cell death, characterized by an increased number of autophagosomes in the cytoplasm; and (3) necrosis, type III cell death. Radiation-induced cell inactivation is considered a concept of senescence-like growth arrest.<sup>5,6</sup>

In vitro, the issue of cell death induced by ionizing radiation in glioblastoma cells has been previously reported;<sup>7,8,9,10,11,12</sup> however, histological analyses of glioblastoma cells after carbon-ion exposure are still limited and ultrastructural characteristics have not been investigated in detail. Here we report the results of conventional morphological analyses, including morphometric and electron microscopic analyses, of cell death and senescence-like growth arrest after exposure to X-ray and ionizing radiation with various doses in a human glioblastoma cell line (CGNH-89) to elucidate the cytological characteristics of glioblastoma cells against carbon-ion irradiation. We used a CGNH-89 cell line in this study, since the cell line had morphological characteristics such as cellular pleomorphism, similar to typical human glioblastoma cells, and could be well-analyzed in morphology and cytogenetics by one of the authors (SI). We expect that the present study will help us to achieve higher therapeutic gain in glioblastoma patients.

## MATERIALS AND METHODS

### Cell line and culture condition

A human glioblastoma cell line, CGNH-89, was established as described previously.<sup>13,14,15</sup> The cells were maintained at 37°C in Eagle's MEM (Nissui, Tokyo, Japan) supplemented with 10% fetal bovine serum (Invitrogen, Grand Island, NY) and 3% L-glutamine in a humidified atmosphere of 5% CO<sub>2</sub> in air. The cells were subcultured by exposing them in 0.05% trypsin when they were confluent and then resuspending in growth medium.

### Irradiation with X-rays as a reference radiation

A cell monolayer grown on 60-mm dishes was irradiated at room temperature (RT) with 0–10 Gy of X-rays at a dose rate of 0.93 Gy/min at a distance of 30 cm by a 140 kVp, 4.5 mA, X-ray machine (Hitachi MBR-1505R, Tokyo, Japan) with a 0.5 mm Al filter, followed by incubation at 37°C in 95% air / 5% CO<sub>2</sub>.

### Irradiation with heavy ions

Exposure to 0–10 Gy of carbon-ions (18.3 MeV/nucleon, LET = 108 keV/μm) was performed at room temperature, as mentioned elsewhere.<sup>16,17,18,19</sup> In brief, medium from the cell monolayer grown on 60-mm dishes was removed prior to irradiation, and the dishes were covered with 8-μm-thick Kapton polyimide film (DuPont-Toray, Tokyo, Japan) to avoid drying. Soon after irradiation, fresh medium was added to the dishes, and the cultures were subsequently maintained at 37°C in 95% air/5%CO<sub>2</sub>. LET at the cell surface was calculated according to kinetic energy loss, assuming water equivalence. The absorbed dose (Gy) was calculated as fluence (number of ion particles/cm<sup>2</sup>) × LET (keV/μm) × 1.602 × 10<sup>-9</sup>.

### Cell survival analysis

Cell survival was determined by the colony formation assay as follows: Within 1 h post-irradiation, confluent cultures were rinsed with phosphate-buffered saline (PBS) and trypsinized. The cells were counted and reseeded into 60-mm dishes. After incubation for 7 days, colonies were fixed in methanol, stained with Giemsa solution and counted. Only colonies containing more than 20 cells were counted as survivors. The surviving fraction in colonies was plotted on a semilog scale as a function of the dose.

### Histological analysis

For each group (0-10 Gy), cells were fixed in formalin, and stained with hematoxylin-eosin (HE).

### Cell count

Under a microscope, more than 1000 nuclei were counted on each slide. Counting was performed using a 10 × 10 square grid eyepiece graticule at ×100. Cell numbers were compared on average per 1 mm<sup>2</sup>.

### MIB-1 LI

For immunohistochemical staining with MIB-1 antibody (Dakocytomation, Glostrup, Denmark), we used a streptavidin-biotin-peroxidase system kit (Histofine SAB-PO kit, Nichirei, Tokyo, Japan). After the cells were fixed in ethanol for 30 minutes, they were incubated with MIB-1 antibody (1:100) for 30 minutes at RT. The slides were counterstained with hematoxylin. The labeling index (LI) of

MIB-1 was defined as the percentage of immunostained nuclei divided by the total number of 1000 nuclei in the field of maximal labeling. Only distinct immunoreactivity was considered MIB-1 positive.

### Nuclear measurements

HE-stained slides were viewed at low magnification under a microscope. We chose five fields that showed diffuse cellularity on 3 samples. We then digitized a single microscopic field ( $\times 20$  objective) with a charge-coupled device camera (NIKON DS-5M, Tokyo, Japan.). The area of the digitized image was set at  $640 \times 480$  pixels (1 pixel =  $0.456 \mu\text{m}^2$  of a slide) and saved in full-color (24 bits RGB) BMP format. Nuclear segmentation (identification) and morphometric measurements were performed using public domain software (Gunmetry, <http://sos.sourceforge.jp/>), coded

in JAVA (Sun Microsystems, Santa Clara, CA, USA).<sup>20,21</sup>

### Electron microscopy

CGNH-89 cells were fixed at various time points after irradiation. Irradiated and non-irradiated control specimens were fixed with a fixative containing 1% glutaraldehyde, 1.6% formaldehyde, 0.1 M phosphate buffer, pH 7.4. After washing with 7% sucrose, 0.1 M phosphate buffer, pH 7.4, they were post-fixed with 2% osmium tetroxide, 0.1 M phosphate buffer, pH 6.8. They were then dehydrated by passage through a graded ethanol series and embedded in Quetol 812 (Nisshin EM, Tokyo, Japan). Ultrathin sections were cut, stained with uranium acetate and lead citrate, and examined by transmission electron microscopy (JEM-200CX; JEOL Ltd., Tokyo, Japan).

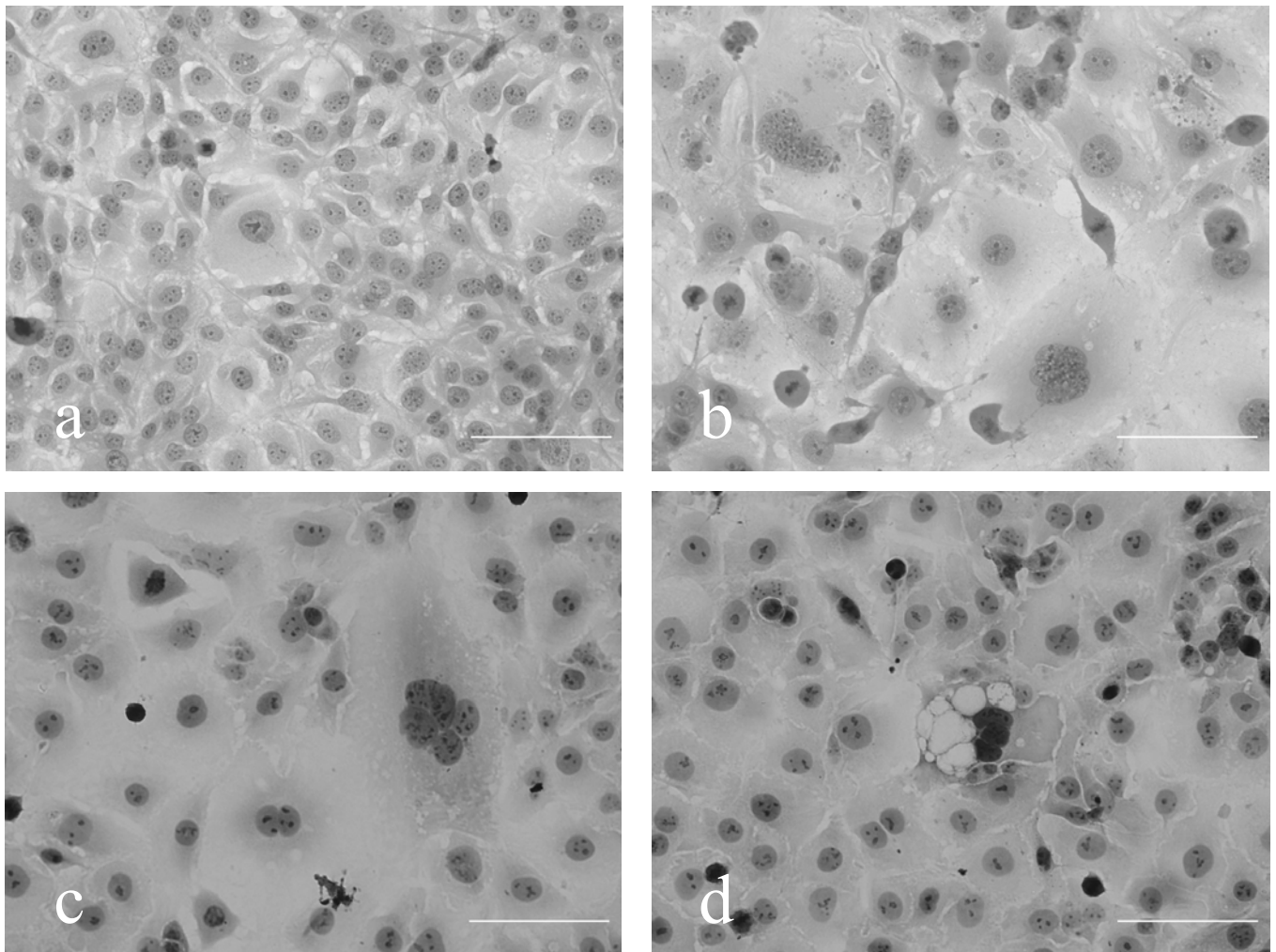


**Fig. 1:** Light microscopic images of human glioblastoma CGNH-89 cells. (a) Control cells seeded after 48 hours are highly cellular and relatively monotonous with slight nuclear pleomorphism, marked nuclear atypia and brisk mitotic activity. See multinucleated giant cells. (b) After 48 hours' X-ray exposure to 10Gy, living cells show cytomegalia, nuclear condensation, the increase of atypical mitotic figures and cytoplasm with a tendency to increase in size. (c)(d) After 48 hours' carbon-ion exposure to 10 Gy, living cells show atypical mitosis (c) and intracytoplasmic vacuoles (d) in addition to similar changes of X-ray exposure. a-d, HE staining. Scale bar = 100  $\mu\text{m}$ .



### DNA Direct sequence

TP53 mutations in the DNA from non-irradiated CGNH-89 were analyzed by direct sequencing. PCR amplification (denaturing 95°C, 30s; annealing 60°C, 30s; extension 72°C, 30s; 35 cycles) using cDNA (TP53 exon 5,6,7 and 8) as a

template from CGNH-89 cells, was directly sequenced using a BigDye Terminator v3.0 Cycle Sequencing Ready Reaction Kit (Applied Biosystems). Then, we automatically detected TP53 mutations using an ABI PRISM3100 sequencer.

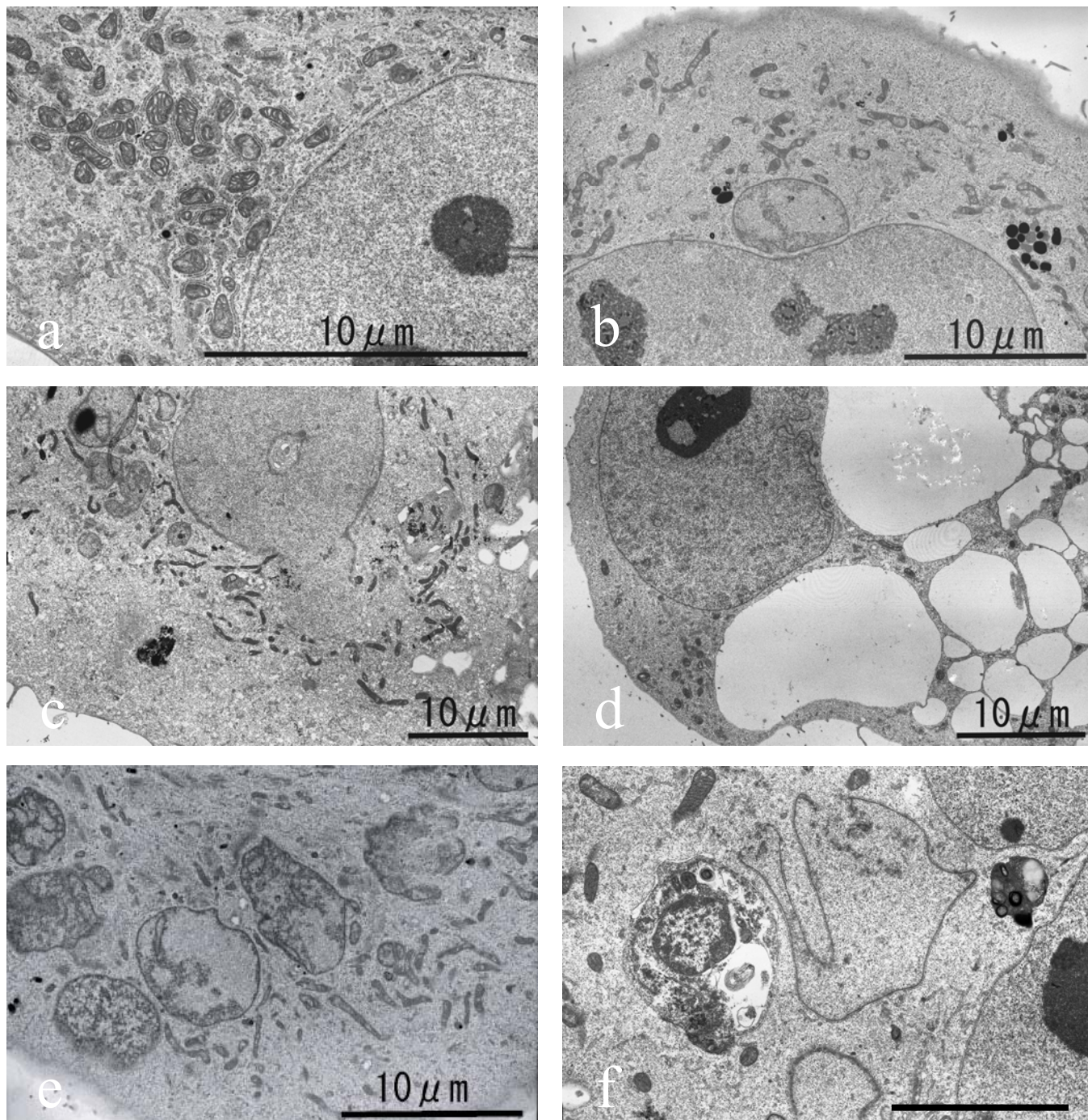


**Fig.2:** Ultrastructure of CGNH-89 cells. (a) Control cells usually have prominent nucleolus, many cytoskeleton, some vacuoles and many normal mitochondria with fine cristae, many endoplasmic reticulum, many Golgi apparatus, and few lysosomes in the cytoplasm. (b) After 48 hours X-ray exposure to 10Gy, cellular enlargement seems to depend on swelling of mitochondria, increased cellular organelles, cytoskeleton and some lysosomes. Nuclear membrane is slightly indented. (c-f) After 48 hours' carbon-ion exposure to 10 Gy, living cell nuclei and cytoplasm after exposure show a tendency to increase in size. We observe large cells consisting of vacuolation, swelling of mitochondria, increased cellular organelles, cytoskeleton, and secondary lysosomes (c). Note the many intracytoplasmic vacuoles (d), numerous swollen mitochondria with the expansion of matrix, a few coarse cristae and vesicular shape (e), and some electron dense bodies of secondary lysosomes in large cells (f). Scale bar = 10 μm.

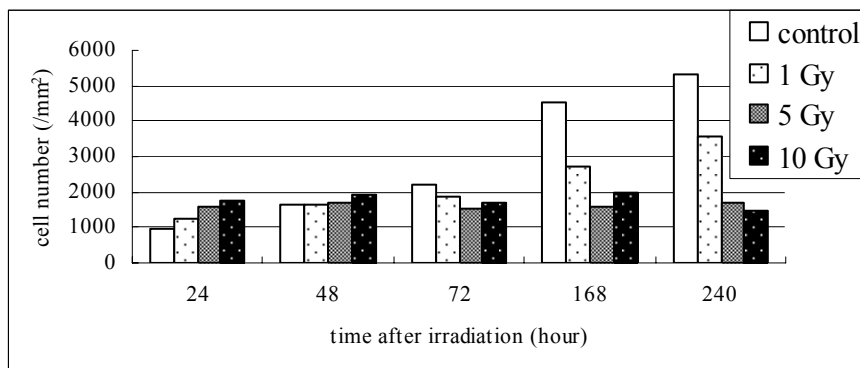


**Fig. 3:** Cell counts per 1mm<sup>2</sup> of CGNH-89 cells before and after irradiation. In non-irradiated cells, cell numbers increase over time. In irradiated cells, cell numbers show a tendency to decrease dependently dose over time. Control: non-irradiated CGNH-89 cells. 1Gy, 5Gy, and 10Gy: CGNH-89 cells irradiated by carbon-ion of 1 Gy, 5 Gy and 10 Gy.

### Statistical analysis

The cell number, nuclear area size, and MIB-1 LI data represent the average of several independent assays. Student's t-test was used for statistical analysis, and differences at  $p < 0.05$  were considered to be significant.

## RESULTS

### Character of CGNH-89 cells

Human glioblastoma CGNH-89 cells had nuclei with pleomorphism, marked nuclear atypia and brisk mitotic activity. Most cells were highly cellular and monotonous, while some were multinucleated giant cells (Fig. 1a). Ultrastructurally, control CGNH-89 cells usually had some vacuoles and many normal mitochondria with fine cristae in the cytoplasm (Fig. 2a). Cell population increased over time by about two-fold between day 2 and day 4. In a dish, cell population and cellularity increased, so the per unit area saw an increase in the number of nuclei (Fig. 3). By morphometric analysis of the nuclear size, the mean nuclear area decreased after 48 hours over time (Fig. 4a). MIB-1 LI showed little change from 0 to 48 hours (Fig. 5). Sequence analysis confirmed that CGNH-89 cells had a G to A transition in codon 280 in exon 8 of the TP53 gene (data not shown).

### X-ray exposure

After X-ray exposure, living cells decreased in number (data not shown). Microscopically, the cells showed nuclear condensation, an increase of atypical mitotic figures and a tendency of increase in cytoplasm after exposure (Fig. 1b). MIB-1 LI decreased in the 24 hours after exposure, but increased in 48 hours (Fig. 5). Ultrastructurally, cellular enlargement seemed to depend on the swelling of mitochondria

and increase of cellular organelles and cytoskeleton (Fig. 2b).

### Carbon-ion exposure

After carbon-ion exposure, living cells decreased in number (Fig. 3, 5). The colony forming assay showed a linear relationship on a semi-log plot between the dose and surviving fraction (Fig. 6). In HE staining, in addition to similar changes in X-ray exposure (Fig. 1c,d), we could observe almost dead cells floating in the medium in a dish in a short time (post-irradiation, ~24 h). Morphometrically, the nuclei and cytoplasm after carbon-ion exposure showed a tendency to increase in size (Fig. 4b). The deviation of nuclear area size increasing during 48 hours after irradiation, and the small/large ratio shifted to higher in 336 hours. (Fig. 4b, c) After exposure (control, 5Gy, 10Gy), MIB-1 LI decreased in 24 hours (12%, 11%, 7%) but increased in 48 hours (10%, 20%, 21%), respectively (Fig. 5).

Ultrastructurally, the cells exhibited similar changes to X-ray-irradiated cells (Fig. 2c). Moreover, carbon-ion treatment induced additional changes such as nuclear expansion, enrichment of nuclear chromatin and increased atypical nuclei, and finally increased multinucleated cells. On the other hand, after exposure, the vacuolation expanded and increased (Fig. 2d). After irradiation, the cells contained swollen mitochondria with expanded matrix spaces and fewer cristae (Fig. 2e). Although cytoskeletal filaments had no deviation in intracellular distribution, the enlarged cytoplasm after exposure consisted of increased cytoskeletal filaments (Fig. 2c). We observed increased secondary lysosomes, a few of which included damaged organelle (Fig. 2f).

In this study, we could not find apoptotic bodies by light or electron microscopy.

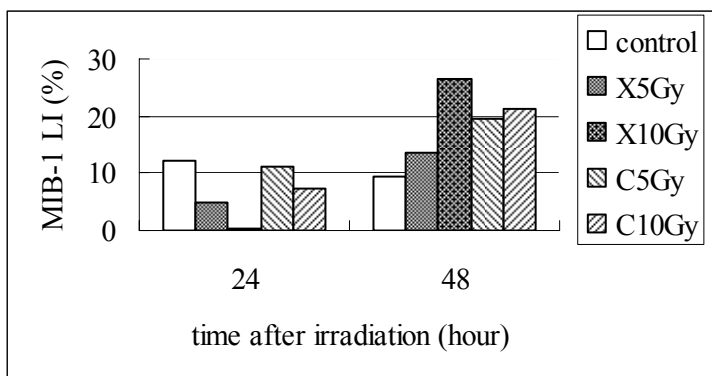
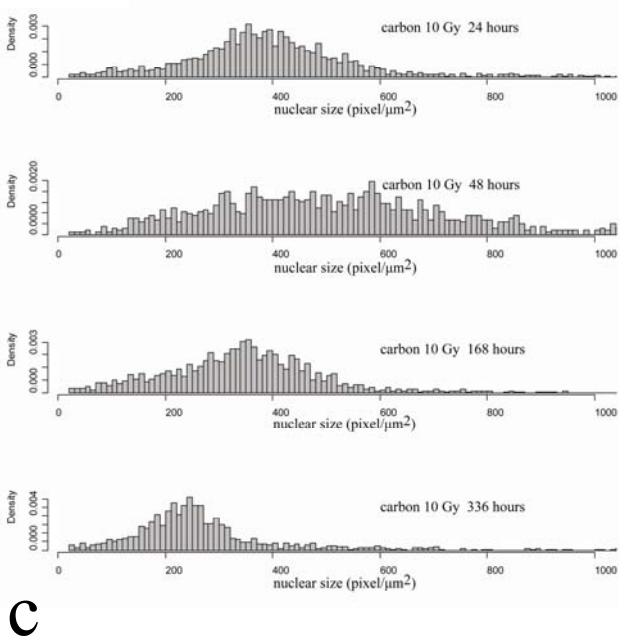
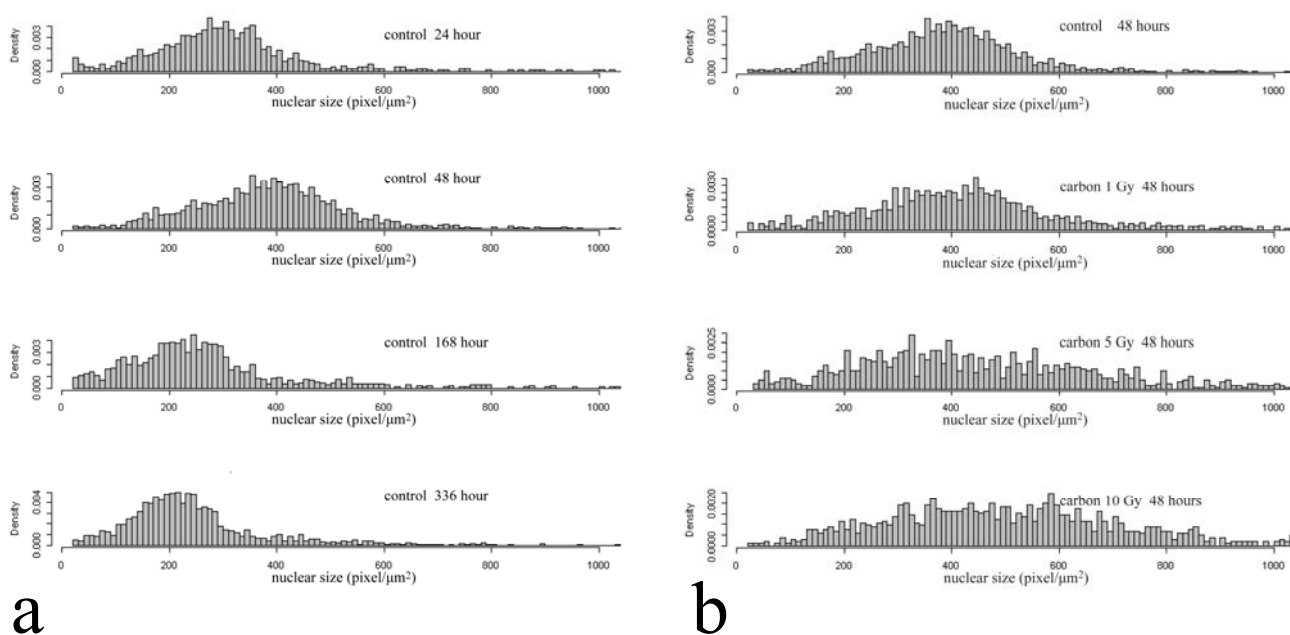


**Fig. 4:** Nuclear area size histogram of CGNH-89 cells. (a) In non-irradiated CGNH-89 cells, over time, the density of small nuclear area size is high. (b) In CGNH-89 cells irradiated by carbon-ion at 48 hours, with dose response, the deviation of the nuclear area size show a tendency to increase dose dependently. (c) In CGNH-89 cells irradiated by 10 Gy carbon-ion, at 48 hours the deviation of the nuclear area size is greatest, and then at 336 hours, the density of the small nuclear area size is as high as non-irradiated cells. The density of irradiated cells shows a significant change from 48 hours to 336 hours.

**Fig. 5:** MIB-1 labeling index (LI) of CGNH-89 cells before and after irradiation at 24 hours and 48 hours. At 24 hours, LI show a tendency to decrease by X-ray and carbon-ion exposure compared to the control. At 48 hours, LI show a tendency to increase with both exposures compared to the control. LI by both X-ray and carbon-ion exposure shows no significant difference. Control: non-irradiated CGNH-89 cells. X5Gy: CGNH-89 cells irradiated by X-ray of 5 Gy. X10Gy: CGNH-89 cells irradiated by X-ray of 10 Gy. C5Gy: CGNH-89 cells irradiated by carbon-ion of 5 Gy. C10Gy: CGNH-89 cells irradiated by carbon-ion of 10 Gy.



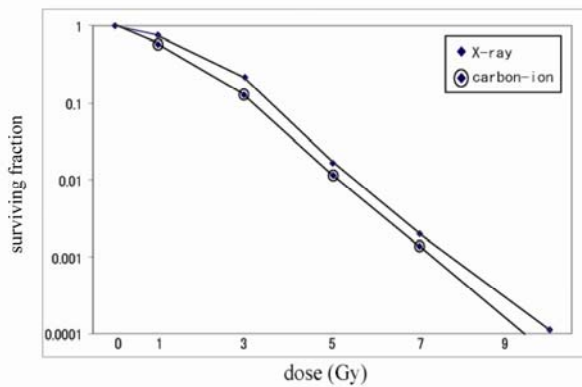


**Fig. 6:** Colony forming assay/ surviving fraction in irradiated CGNH-89 cells. The survival fraction of both treatments similarly decreases in a dose-dependent manner. Diamond and diamond-circle symbols represent X-ray and carbon-beams, respectively.

## DISCUSSION

The heavy ion-induced changes in CGNH-89 cells observed in the present study were as follows: 1) decreased cell number, 2) diversity of nuclear area size, 3) occurrence of large or giant cells, 4) swollen mitochondria, 5) occurrence of secondary lysosomes, 6) in the later stages, increased small tumor cells. The changes with carbon-ion seemed to be slightly higher than those with X-ray. In our study, the decrease of glioblastoma cells by X-ray and carbon-ion irradiations was likely to indicate cell death. Glioblastoma cell killing after X-ray and heavy-ion irradiation remains to be clarified, although *in vitro* cytotoxicity of X-ray and carbon-beams against glioblastomas, which are clinically resistant to radiation therapy, has previously been analyzed.<sup>7,8,9,10,11,12</sup> Our results that the decrease in glioblastoma cells by X-rays and carbon-ion irradiation was dose dependent were similar to the above reports. Our morphological analyses of surviving or remaining cells failed to demonstrate complete pictures of cell death, such as apoptosis, autophagy or necrosis, in glioblastoma cells at the point of study. However, the

present study showed nuclear and cytoplasmic expansion, swollen mitochondria and secondary lysosomes at the level of electron microscopy in glioblastoma cells irradiated by carbon-beam. Based on the morphological findings with cell loss data, the major cell death of CGNH-89 cells was considered as so-called type II and type III cell death, but not apoptosis, type 1 cell death, at doses from 1 to 10 Gy. Yao et al. reported that autophagic cell change, instead of apoptosis, occurred in 6 glioblastoma cell lines following gamma irradiation.<sup>8</sup> Iwadate et al. reported that neither U87 nor T98 GBM cell lines demonstrated apoptosis in response to

irradiation.<sup>11</sup>

The reason why apoptosis was hardly observed in this study might be the observation time point, which did not correspond to the peak of apoptosis in irradiated cells of various types. In general, radiation-induced apoptosis occurred in glioblastoma cells with wild-type (wt) TP53, but only a little apoptosis occurred after X-ray irradiation in glioblastoma cells with mutant (mt) TP53.<sup>22</sup> However, the maximum apoptotic indices were obtained on day 10 (240 hours) after 80 keV/ $\mu\text{m}$  carbon-beam irradiation in cell lines including glioblastoma (independent of TP53 status).<sup>12</sup> Therefore we thought that we did not observe apoptosis in our cell line, CGNH-89, with mutated TP53, during 4 days, from day 1 to day 4, after 108 keV/ $\mu\text{m}$  carbon-beam irradiation.

Our ultrastructural study showed “large” cells with mitochondrial transformation or swelling, and secondary lysosomes after X-ray or carbon-beam exposure. Concerning the type or origin of the large cells, we considered two possible types, “senescence cells” or “unclassified dying cells”. In a previous report,<sup>23</sup> so-called monstrous or giant cells with multinucleated, degenerated nuclei appeared in human glioblastomas by X-ray irradiation, and this type of cell is considered as non-proliferating cells. Instead, regrowth and relapse was caused by the proliferation of small neoplastic cells. Hamada et al. reported that normal fibroblasts changed giant, multinucleated cells like senescence after exposure to carbon-ions.<sup>16</sup> In a previous report,<sup>24</sup> neoplastic cells in glioblastoma tissues after radiation therapy appeared to enlarge or show cellular pleomorphism without proliferating potential. In this study, with the occurrence of large cell peaks at 48 hours after irradiation, and after these peaks, the large/whole cell ratio decreased. Morphometrical analysis of nuclear size in the present study suggested that the “large” cells did not proliferate. Thus, these “large” cells were unlikely to be the main cell type with proliferating potential. These “large” cells clearly differed from tumor cells of the giant cell glioblastoma (GCG), WHO grade IV since, ultrastructurally, GCG did not have swollen mitochondria or secondary lysosomes.<sup>25</sup> From the morphological point of view, it is difficult to distinguish whether “large” cells were a change into cell death or a change that keeps dividing as degeneration.

One of the characteristic findings observed in this ultrastructural study were the changes of mitochondria, probably indicating degeneration as senescence, in these large cells. The swollen mitochondria caused by irradiation suggested a relation to cell enlargement. Alterations in the structure and function of mitochondria are commonly observed by irradiation in a wide variety of cells as follows: elongation and branching of the mitochondria, a reversible increase of

their size including the development of giant forms, increased number of mitochondria, vacuolization, and disruption of the outer and inner membranes of mitochondria.<sup>26</sup> We observed the above form of mitochondrial change in the “large” cells, ultrastructurally. The change of mitochondria was reported as it related to the inducement of PCD<sup>27, 28, 29, 30, 31</sup> and senescence.<sup>5</sup> Correlated three-dimensional light and electron microscopic study revealed transformation of mitochondria to vesicular or swollen forms during apoptosis,<sup>32</sup> but our ultrastructural study failed to detect other apoptotic nuclear and cytoplasmic changes in the large cells. Mitochondrial changes unrelated to PCD should also be considered to occur after X-ray and carbon-beam irradiations.

On the other hand, our results that, following carbon-beam radiation, the number and the volume fraction of lysosomes increased in CGNH-89 cells were similar to a previous finding in a variety of cell types after ionizing radiation.<sup>26, 29</sup> Furthermore, expansion of the lysosomal compartment was due to the accumulation of undegraded material as a consequence of the decreased rate of lysosomal protein degradation in irradiated cells.<sup>26</sup> However, the present study failed to detect autophagic cell death, although our ultrastructural study showed autophagic vacuoles in the “large” cells; therefore, we considered the phenotype of the “large” cells as senescence.

In this study, MIB-1 LI of irradiated cells showed a tendency to decrease in 24 hours and to increase in 48 hours compared with the control. Additionally, small cells appeared in the later stage, and contributed to the increase of total cell number and regrowth, and the small/total cell ratio greatly increased. It is suggested that X-ray and carbon-beam irradiation triggered synchronization the cell cycle. Wada et al. mentioned the DNA double-strand break (DSB) caused by heavy-ion irradiation,<sup>33</sup> and Hamada et al. suggested repair of DNA damage, since they found that the number of phosphorylated H2AX foci detecting DNA damage caused by radiation-induced DSB decreased over a short time.<sup>34</sup> Short et al. reported that three mt TP53 glioma cell lines exhibited marked, Rad51-dependent repair and G2 checkpoint activation after low radiation doses.<sup>35</sup> Takahashi et al. described that tumor cells were recruited from the quiescent phase into the cell cycle after irradiation.<sup>36</sup> All these reports suggested that the cell cycle was recruited to repair DNA damage. Our data, both the decrease of cell number and the increase of MIB-1 LI suggested the cell cycle without proliferation was induced by irradiation exposure. The cell cycle without proliferation might be related to DSB by irradiation and repair of the DSB. Combining our findings with a report by Castedo M et al.<sup>30</sup>, we considered that tumor cells that survived after 48 hours’ irradiation may divide into two types of cells; large cells with low proliferating potency and other proliferating or quiescent

small cells with radiation resistance.

We concluded that carbon-ion irradiation induced cell death and senescence in a glioblastoma cell line with mt TP53. Morphologically, novel findings were as follows: increased large cells, enlarged and bizarre nuclei, swollen mitochondria, and secondary lysosomes. This study also indicated that small cells survived the irradiation were an important player for proliferation and regrowth of glioblastoma. As for further analysis, it is recommended to evaluate cell death of other glioblastoma cell lines with various TP53 status by light and electron microscopy after carbon-ion beam exposure. Although there was little difference in the cellular effect compared with X-ray, we hope that carbon-ion beam therapy has an advantage of being that more effective against neoplasms (e.g., glioblastoma) than normal brain tissue (e.g., neuron, glia, endothelial cells and so on).

## ACKNOWLEDGMENTS

We thank Machiko Yokota, Koji Isoda, Hiroko Yamazaki, Hiroyuki Seo and Kiyoko Takahashi (Gunma University, Japan) for assistance with TEM and immunohistochemical staining. Thanks are also due to the staff at TIARA of JAEA for help with heavy-ion irradiation. This work was supported by a Grant-in-Aid for the 21st Century Center of Excellence Program for Biomedical Research Using Accelerator Technology, by Grants-in-Aid for Scientific Research (B)(Y.N. no. 19300123), and Grants-in-Aid for Exploratory Research (Y.N. no. 18650096) from the Ministry of Education, Culture, Sports, Science, and Technology of Japan.

## REFERENCES

1. Kleihues P, Burger PC, Aldape KD et al. Glioblastoma. In: Louis DN, Ohgaki H, Wiestler OD, Cavenee WK (eds), *World Health Organization Classification of Tumours of the Central Nervous System* (4th edn). Lyon: IARC 2007; 33-49.
2. Ohgaki H, Dessen P, Jourde B, et al. Genetic pathways to glioblastoma: a population-based study. *Cancer Res* 2004; **64**: 6892-6899.
3. Mizoe J, Tsujii H, Hasegawa A, et al. Phase I/II clinical trial of carbon-ion radiotherapy for malignant gliomas: combined X-ray radiotherapy, chemotherapy, and carbon ion radiotherapy. *Int J Radiat Oncol Biol Phys* 2007; **69**: 390-396.
4. Takahashi T, Mitsuhashi N, Furuta M, et al. Apoptosis induced by heavy ion (carbon) irradiation of two human tumours with different radiosensitivities in vivo: relative biological effectiveness (RBE) of carbon beam. *Anticancer Res* 1998; **18**: 253-256.
5. Suzuki M, Suzuki K, Kodama S, Watanabe M. Interstitial chromatin alteration causes persistent p53 activation involved



*Glioblastoma cells after carbon-beam exposure*

in the radiation-induced senescence-like growth arrest.

*Biochem Biophys Res Commun* 2006; **340**: 145-150.

6. Krtolica A, Campisi J. Cancer and aging: a model for the cancer promoting effects of the aging stroma. *Int J Biochem Cell Biol.* 2002; **34**: 1401-1414.

7. Quick QA, Gewirtz DA. An accelerated senescence response to radiation in wild-type p53 glioblastoma multiforme cells. *J Neurosurg* 2006; **105**: 111-118.

8. Yao KC, Komata T, Kondo Y, Kanzawa T, Kondo S, Germano IM. Molecular response of human glioblastoma multiforme cells to ionizing radiation: cell cycle arrest, modulation of the expression of cyclin-dependent kinase inhibitors, and autophagy. *J Neurosurg* 2003; **98**: 378-384.

9. Stapper NJ, Stuschke M, Sak A, Stüben G. Radiation-induced apoptosis in human sarcoma and glioma cell lines. *Int J Cancer.* 1995; **62**: 58-62.

10. Tsuboi K, Tsuchida Y, Nose T, Ando K. Cytotoxic effect of accelerated carbon beams on glioblastoma cell lines with p53 mutation: clonogenic survival and cell-cycle analysis. *Int J Radiat Biol* 1998; **74**: 71-79.

11. Iwadata Y, Mizoe J, Osaka Y, Yamaura A, Tsujii H. High linear energy transfer carbon radiation effectively kills cultured glioma cells with either mutant or wild-type p53. *Int J Radiat Oncol Biol Phys* 2001; **50**: 803-808.

12. Tsuboi K, Moritake T, Tsuchida Y, Tokuyue K, Matsumura A, Ando K. Cell cycle checkpoint and apoptosis induction in glioblastoma cells and fibroblasts irradiated with carbon beam. *J Radiat Res* 2007; **48**: 317-325.

13. Ishiuchi S, Tsuzuki K, Yoshida Y, et al. Blockage of Ca<sup>2+</sup>-permeable AMPA receptors suppresses migration and induces apoptosis in human glioblastoma cells. *Nat Med* 2002; **8**: 971-978.

14. Ishiuchi S, Yoshida Y, Sugawara K, et al. Ca<sup>2+</sup>-permeable AMPA receptors regulate growth of human glioblastoma via Akt activation. *J Neurosci* 2007; **27**: 7987-8001.

15. Ishiuchi S, Nakazato Y, Iino M, Ozawa S, Tamura M, Ohye C. In vitro neuronal and glial production and differentiation of human central neurocytoma cells. *J Neurosci Res.* 1998; **51**: 526-535.

16. Hamada N, Hara T, Funayama T, Sakashita T, Kobayashi Y. Energetic heavy ions accelerate differentiation in the descendants of irradiated normal human diploid fibroblasts. *Mutat Res* 2008; **637**: 190-196

17. Hamada N, Funayama T, Wada S, et al. LET-dependent survival of irradiated normal human fibroblasts and their descendants. *Radiat Res* 2006; **166**: 24-30.

18. Hamada N, Ni M, Funayama T, Sakashita T, Kobayashi Y. Temporally distinct response of irradiated normal human fibroblasts and their bystander cells to energetic heavy ions. *Mutat Res in press* (doi: 10.1016/j.mrfmmm.2007.11.001).

19. Hamada N, Matsumoto H, Hara T, Kobayashi Y.

Intercellular and intracellular signaling pathways mediating ionizing radiation-induced bystander effects. *J Radiat Res* 2007; **48**: 87-95.

20. Tanaka G, Nakazato Y. Conditional entropy as an indicator of pleomorphism in astrocytic tumors. *Neuropathology* 2004; **24**: 183-193.

21. Scientific Open Source (SOS) project [homepage on the Internet]. Japan: Scientific Open Source (SOS) project [update 19 June 2007]. Available from: <http://sos.sourceforge.jp/>

22. Takahashi A, Ohnishi K, Tsuji K, et al. WAF1 accumulation by carbon-ion beam and  $\alpha$ -particle irradiation in human glioblastoma cultured cells. *Int J Radiat Biol* 2000; **76**: 335-341.

23. Ogashiwa M, Maeda T, Yokoyama H, Takeuchi K, Akai K. [Morphologic findings and biologic behavior in the high grade glioma—a postmortem study of 22 cases][Article in Japanese] *Gan No Rinsho* 1989; **35**: 1297-1307.

24. Burger PB, Scheithauer BW. Glioblastoma. *Tumor of The Central Nervous System* fourth series fascicle 7. Washington, DC: AFIP 2007; 55-77.

25. Liberski PP, Kordek R. Ultrastructural pathology of glial brain tumors revisited: a review. *Ultrastruct Pathol* 1997; **21**: 1-31.

26. Somosy Z. Radiation response of cell organelles. *Micron.* 2000; **31**: 165-181.

27. Frank S, Oliver L, Lebreton-De Coster C, et al. Infrared radiation affects the mitochondrial pathway of apoptosis in human fibroblasts. *J Invest Dermatol.* 2004; **123**: 823-831.

28. Hino M, Wada S, Tajika Y, et al. Heavy ion microbeam irradiation induces ultrastructural changes in isolated single fibers of skeletal muscle. *Cell Struct Funct.* 2007; **32**: 51-56.

29. Bröker LE, Kruyt FA, Giaccone G. Cell death independent of caspases: a review. *Clin Cancer Res.* 2005; **11**: 3155-3162.

30. Castedo M, Perfettini JL, Roumier T, et al. Mitotic catastrophe constitutes a special case of apoptosis whose suppression entails aneuploidy. *Oncogene.* 2004; **23**: 4362-4370.

31. Terman A, Gustafsson B, Brunk UT. The lysosomal-mitochondrial axis theory of postmitotic aging and cell death. *Chem Biol Interact.* 2006; **163**: 29-37.

32. Sun MG, Williams J, Munoz-Pinedo C, et al. Correlated three-dimensional light and electron microscopy reveals transformation of mitochondria during apoptosis. *Nat Cell Biol.* 2007; **9**: 1057-1065.

33. Wada S, Kobayashi Y, Funayama T, Natsuhori M, Ito N, Yamamoto K. Detection of DNA damage in individual cells induced by heavy-ion irradiation with a non-denaturing comet assay. *J Radiat Res (Tokyo).* 2002; **43 Suppl**: S153-156.

34. Hamada N, Schettino G, Kashino G, et al. Histone H2AX phosphorylation in normal human cells irradiated with focused ultrasoft X rays: evidence for chromatin movement during

repair. *Radiat Res.* 2006; **166**: 31-38.

35. Short SC, Martindale C, Bourne S, Brand G, Woodcock M, Johnston P. DNA repair after irradiation in glioma cells and normal human astrocytes. *Neuro Oncol.* 2007; **9**: 404-411.

36. Takahashi T, Nakano T, Oka K, Ando K. Transitional increase in growth fraction estimated by Ki-67 index after irradiation to human tumor in xenograft. *Anticancer Res.* 2004; **24**: 107-110.